



## Full Length Article

## Effects of low-dose gamma radiation on DNA measured using a quartz tuning fork sensor



Reem Alanazi<sup>a</sup>, Khaled Alzahrani<sup>b</sup>, Khalid E. Alzahrani<sup>a,c</sup>, Nadyah Alanazi<sup>a,c</sup>, Abdullah N. Alodhayb<sup>a,c,d,\*</sup>

<sup>a</sup> Department of Physics and Astronomy, College of Science, King Saud University, Riyadh 11451, Saudi Arabia

<sup>b</sup> Department of Clinical Laboratory Sciences, College of Applied Medical Sciences, King Saud University, Riyadh 12372, Saudi Arabia

<sup>c</sup> Biological and Environmental Sensing Research Unit, King Abdullah Institute for Nanotechnology, King Saud University, P.O. Box 2455, Riyadh 11451, Saudi Arabia

<sup>d</sup> Research Chair for Tribology, Surface, and Interface Sciences, Department of Physics and Astronomy, College of Science, King Saud University, Riyadh 11451, Saudi Arabia

## ARTICLE INFO

## Keywords:

Biosensors  
DNA damage  
DNA repair  
DNA strand breaks  
DNA structures  
Radiobiology  
Quartz Tuning Fork

## ABSTRACT

Despite the expected direct effects of radiation on DNA through its direct interaction with the biomolecule, research indicates that radiation also interacts with the DNA's environment, resulting in indirect effects. Therefore, in this study, we explored the feasibility of using the quartz tuning fork (QTF) sensor system in biomedical applications, specifically in detecting DNA damage caused by low doses of gamma radiation, directly and indirectly. We differentiated between direct and indirect damage by analyzing the fork's resonance frequency changes. This experiment was divided into three stages: before, during, and after irradiation. Each stage involved samples of pure DNA and DNA in a 60- $\mu$ L aqueous solution, evaluated under identical conditions. Before irradiation, we measured frequency shifts ( $\Delta f$ ) over a 20-min period, resulting in values of 19.34, 20.25, and 7.6 Hz for water, DNA, and DNA in water, respectively. Subsequently, the samples were irradiated with cesium-137 for the specified duration, resulting in frequency shifts of  $\sim$  39.21, 28.37, and 41.23 Hz for the same conditions. Our investigations showed an increase in  $\Delta f$  from 20.25 to 28.3 Hz at doses ranging from 7.5 to 30  $\mu$ Gy for pure DNA. Interestingly, DNA in aqueous solution exhibited hypersensitivity to radiation, with frequency shifts ranging from 7.6 to 41.23 Hz. Furthermore, we observed a significant difference in frequency shift after irradiation between pure DNA and DNA in water, with shifts of  $\sim$  70.75–98.45 Hz and 56.32–79.28 Hz for DNA and DNA in water, respectively. This result indicates a significant increase in DNA damage in aqueous environments, driven by the generation of active hydroxyl radicals ( $\text{OH}^\cdot$ ), resulting in base damage and an associated increase in strand breaks. Consequently, our research indicates a lack of substantial direct impact on DNA repair owing to the absence of a conducive postirradiation environment. Therefore, QTF is a valuable biomarker for radiation sensitivity and is promising for future applications as a mass-sensitive biosensor.

## 1. Introduction

Life's continuity depends on organisms preserving their genetic data. DNA, the repository of genetic information in cells, is the fundamental basis of inheritance. Moreover, DNA is an exceptional biological material for biosensing owing to its high sensitivity to chemical modifications caused by internal and external factors. Ionizing radiation can alter DNA's structure and functionality, resulting in mutations that contribute to aging, cancer, and various human diseases (Xu, 2019). Biosensors have diverse applications, particularly in healthcare, drug discovery,

and environmental monitoring. Resonator-based biosensors, such as quartz tuning forks (QTFs), are increasingly recognized for biomedical applications. These devices detect biomolecules in air or liquid by converting their mass into signals reflected in the resonant frequency of the QTF. The performance of biosensors depends on factors such as their quality and the interaction between target biomolecules and the resonator's surface during biological analysis (Kaleli-Can, 2021).

Therefore, in recent decades, many studies have explored DNA-based biosensors. Ptasińska et al. (Ptasińska, 2008) conducted pioneering research focusing on strand breaks to initiate radiation-induced DNA

\* Corresponding author at: Department of Physics and Astronomy, College of Science, King Saud University, Riyadh 11451, Saudi Arabia.  
E-mail address: [aalodhayb@ksu.edu.sa](mailto:aalodhayb@ksu.edu.sa) (A.N. Alodhayb).

damage under ultrahigh vacuum (UHV) conditions, specifically addressing direct damage. Meanwhile, Rosenberg et al. (Rosenberg, 2014) investigated the extent of radiation damage in double-stranded DNA (dsDNA) absorbed on gold surfaces and the associated interfacial bonding. Examining the impact of radio-sensitizers such as cisplatin on DNA bond-breaking, Xiao et al. (Xiao, 2013) determined that the increased bond-breaking observed was due to high sensitivity to low-energy electrons (LEE) and enhanced LEE production at the radio-sensitizer binding site. McKee et al. (McKee, May 2019) used X-rays to release LEE from a gold substrate and investigated the resulting damage in model systems of condensed nucleotides. This methodology was further refined by Kundu et al. (Kundu, 2020), who integrated a separate LEE source to assess damage to deoxyadenosine monophosphate using X-ray photoelectron spectroscopy. Although these investigations primarily focused on direct damage caused by X-ray photons and LEEs under UHV conditions, Faraj et al. reported significant DNA damage induced by X-rays and  $\gamma$ -rays. Therefore, it is concluded that DNA damage depends on the dose and dose rate, making it a promising biomarker for radiation response (Faraj Akram, 2011). Sudprasert et al. assessed the effects of low-dose gamma radiation on DNA damage, chromosomal aberration, and the expression of DNA repair genes in both whole blood and peripheral lymphocytes. Their findings showed a substantial increase in DNA strand breaks and oxidative base damage at sites susceptible to the enzyme formamidopyrimidine-DNA-glycosylase (FPG) owing to radiation exposure (Sudprasert, 2006). For example, in an earlier study, Charlton et al. (1989) calculated the direct interactions between radiation tracks and DNA. However, they did not include the effects of water radicals, such as hydroxyl radicals, generated by ionization and excitations around the DNA. The current computations span time domains from  $10^{-15}$  to  $10^{-9}$  s, covering various stages of radiation's interaction with DNA in a cellular environment. This refined model considers radical lifetimes, providing a more sophisticated understanding of ionizing radiation's impact on DNA (Nikjoo et al., 1997).

Radiation exposure, even at low doses, can damage DNA by causing single-stranded breaks (SSBs), double-stranded breaks (DSBs), and changes in DNA bases, ultimately leading to cell death (Alexandros and Georgakilas, 2020). Chromosome and chromatid breakage are common indicators of chromosomal abnormalities caused by ionizing radiation. Effective repair mechanisms are crucial for proper chromosome pairing and cell division. Failure to repair damage can result in cell death or offspring with genetic abnormalities, especially when both DNA strands are simultaneously damaged (Budak, 2020). Despite this, DNA repair pathways effectively remove most DNA lesions that would otherwise cause mutations or disrupt critical metabolic functions such as replication and transcription, leading to senescence and cell death (Chatterjee and Walker, 2017). Biological repair mechanisms facilitated by DNA repair enzymes are more efficient at addressing single-strand breaks than DSB. However, protective mechanisms should be activated to mitigate radiation dangers. Studies indicate that cells exposed to radiation during mitosis undergo a relatively shorter repair period, typically fixing single-strand breaks in 0.3–3 h. Compared to tumor tissue, normal tissue demonstrates a superior recovery capacity (Budak, 2020).

In this study, we use sensors (specifically QTF technology) in biological applications to assess the extent of DNA damage induced by low doses of cesium-137 gamma radiation. The QTF technique is used to establish a mass-sensitive platform by immersing the QTF fork in three different samples: pure DNA, DNA in deionized (DI) water solution, and DI water alone. The investigation follows a three-stage process: the preirradiation stage, the irradiation stage, where damage occurs, and the postirradiation stage, where repair is attempted. Each stage is applied to all samples under identical conditions. Throughout these stages, the QTFs are monitored to track changes in their resonance frequency over time, indicating DNA damage. Consequently, the changes in resonance frequency observed using the QTF technique are crucial for assessing DNA damage in biomedical applications.

## 2. Methodology

### 2.1. The human DNA model

DNA, located in a cell's nucleus, is composed of nucleotides, each consisting of a phosphate group, a sugar molecule, and one of four nitrogenous bases: adenine (A), thymine (T), guanine (G), and cytosine (C). These bases form the genetic code, providing instructions for the cell's development, functioning, and reproduction (de la Fuente Rosales, 2018). Genes, which are sequences of these bases, are the cell's language, directing protein production. Nucleotides bond together to create two intertwined strands, forming a double helix structure, where adenine pairs with thymine and guanine pairs with cytosine. DNA coils into chromosomes, which contain DNA sequences in a cell. Humans have twenty-three pairs of chromosomes in each cell's nucleus (Qasim and Ahmed, 2020).

### 2.2. Biological effects of radiation

Free radicals, such as hydroxyl radicals and superoxide anions, are highly reactive compounds characterized by an unpaired electron. Ionizing radiation, particularly photon irradiation, triggers water radiolysis, producing free radicals that can indirectly damage DNA. Reactive compounds, including hydrogen peroxide and hydroxyl ions, are also generated (Moreels, 2020). Radiation affects cells through two proposed mechanisms: direct and indirect, as shown in Fig. 1 (Gong et al., 2021). Depending on the cumulative energy transferred to a material, this energy may be high (as in alpha rays) or low [as in long-distance energy transfer (LET) (beta and gamma rays)] (Chatterjee and Walker, 2017). Through the direct effect, gamma rays can transmit both low and high energy via LET. They collide with atoms or molecules, dislodging electrons and inducing ionization. This can cause DNA fractures, including breaks in phosphodiester bonds or the opening of purine rings, affecting single- or double-stranded DNA. However, because ~ 80 % human body cells comprise water, the probability of direct DNA interaction is low

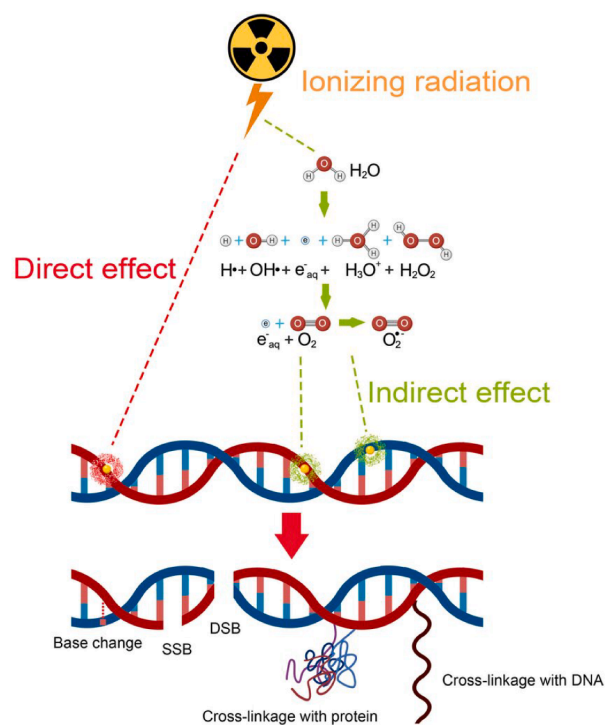
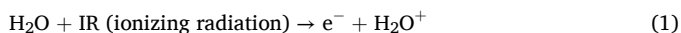


**Fig. 1.** Mechanisms of IR: direct interaction damages DNA, while indirect effects generate free radicals from cellular molecules such as water, resulting in DNA damage (Gong et al., 2021).

when exposed to ionizing radiation because DNA constitutes only 1 % of the cell (Wang, 2019). Approximately 65 % radiation-induced DNA damage is attributed to indirect effects caused by hydroxyl radicals. In this process, radiation ionizes molecules, producing free radicals that interact with DNA, leading to toxic effects and changing its chemical properties (Budak, 2020).

Equation (1) illustrates the disintegration of water under radiation (radiolysis), which creates four free radical products:  $\text{H}\cdot$ ,  $\text{OH}\cdot$ ,  $\text{H}^+$ , and  $\text{OH}^-$ :



Based on this reaction, free radicals from rapid structural breakdown interact with nearby molecules, leading to DNA damage such as cross-linking and DSB (McKee, May 2019). These destructive reactions activate DNA repair mechanisms, which typically effectively address single-strand breaks. However, repairing DSB is more challenging and can lead to errors during rejoining, such as mutations, chromosomal aberrations, or cell death (Kaleli-Can, 2021; Budak, 2020). DSBs are crucial for assessing radiosensitivity and quantifying chromosomal abnormalities following radiation exposure, making them valuable biological dosimeters (Moreels, 2020).

### 2.3. QTF sensors

QTFs represent a significant advancement in sensor technology for measuring mechanical, electrical, optical, and thermal parameters (Zhang, 2018). They find broad applications in chemistry and biology (Voglhuber-Brunnmaier, 2019), including acoustic microscopy (SAM), dynamic force spectroscopy, and scanning electron microscopy for high-resolution topographic analysis (Alshammari, 2020). QTFs are also integral to photothermal-acoustic spectroscopy for bioassays, petrochemical analysis, and environmental studies. Additionally, quartz-enhanced photoacoustic spectroscopy is used for gas sensing. Despite the inherent stability of QTFs owing to their physical characteristics, environmental conditions such as temperature, pressure, humidity, and gas density can experience rapid fluctuations (Rousseau, 2019).

Specifically, numerous experimental results confirm the exceptional sensitivity of QTFs to radiation, rendering them ideal for monitoring low-dose radiation in small rooms and laboratories. High levels of gamma irradiation can induce shifts in the resonance frequency of quartz resonators (Alanazi, 2022). For example, Shimoda et al. (Shimoda and Uno, Jan. 1988) explored the relationship between frequency shifts and gamma radiation, while Alanazi et al. (Alanazi et al., 2021) exposed gold-coated QTFs to gamma radiation from a cesium-137 source. They assessed the sensitivity of QTFs to radiation at various time intervals (0, 1, and 2.5 h) under consistent ambient conditions, revealing increased frequency shifts, with resonance frequencies increasing from 31 to 34.5 kHz for the QTFs. Alanazi et al. (Alanazi, 2023) also showed the reliability of QTFs in evaluating the enhancement of DNA damage at different concentrations of gold nanoparticles (GNPs) during irradiation, highlighting potential biomedical applications. Introducing GNPs during irradiation resulted in higher fork displacement frequencies, suggesting substantial enhancement in damage ratios. At 15  $\mu\text{g/mL}$ , radiotherapy efficacy was significantly enhanced, underscoring the potential for integrating GNP-mediated radiosensitization with sensing technology.

This study employed the Quester Q10 commercial instrument (Fourien Inc., Canada), known for its high quality factor piezoelectric transducer consisting of a QTF with two vibrating prongs made of quartz. The 300 nm thick prongs are coated with silver electrode films

and measure 3.73 mm in height and 0.52 mm in width, with a 0.3 mm gap between them (Fig. 2 (Alanazi et al., 2021)). Equipped with an impedance analyzer, analog-to-digital converters, amplifiers, a controller, and a signal generator capable of conducting frequency sweeps, we recorded the QTF's impedance response at a sampling rate of 0.5 million samples per second. The data acquisition system provided results in a comma-separated value format, which we analyzed using MATLAB, Origin Lab, and Python. Further system details are described in a previous study (Alodhayb, 2020). With the assistance of a piezoelectric material, quartz forks responding to a mechanical signal transform it into electrical excitations, resonating at frequencies of 32,758 Hz under vacuum conditions. When stimulated by a self-excitation setup, the forks exhibit lateral movement. The applied driving voltages to the QTFs during excitation range from 0.1–0.2 V. Consequently, introducing external mass loading is expected to affect the characteristic resonance frequency of QTFs, resulting in a damping effect on the oscillation frequency. However, increasing the mass on the quartz prongs of QTFs should cause a more significant negative shift in resonance frequency (Kaleli-Can, 2021).

### 2.4. Damage and repair mechanisms

DSBs in DNA are repaired by two primary processes: homologous recombination (HR) and nonhomologous end-joining (NHEJ). HR is error-free and occurs during the S and G2 phases, using the sister chromatid as a template. Error-prone NHEJ operates at any cell cycle phase (Duncan and Swensen, 2016). Specific molecules identify and repair altered DNA structures induced by IR triggered by specific genes. A damage checkpoint recognizes changes and activates pathways to protect the genome, known as DNA damage repair (Jia, 2021). Minor lesions, single-strand breaks, or noncomplex DSBs are repaired through nucleotide excision repair, base excision repair (BER), and NHEJ (Yousefzadeh et al., 2021).

Ataxia telangiectasia mutated (ATM), located on human chromosome 11q, plays a crucial role in various cell cycle checkpoints (G1–S, S, and G2–M). It is essential for identifying and repairing DNA damage. Minor DNA damage from low-dose radiation can typically be repaired with ATM, restoring function. However, high doses can cause severe denaturation, leading to challenging-to-repair DNA DSBs and potential cancer risks (Jia, 2021). A study assessing phospho-S1981 ATM levels in control cells demonstrated a significant increase just 15 min after 2 Gy irradiation, initiating repair signaling shortly after DNA damage induction (Blimkie, 2014). Yang et al. observed the dynamic repair process

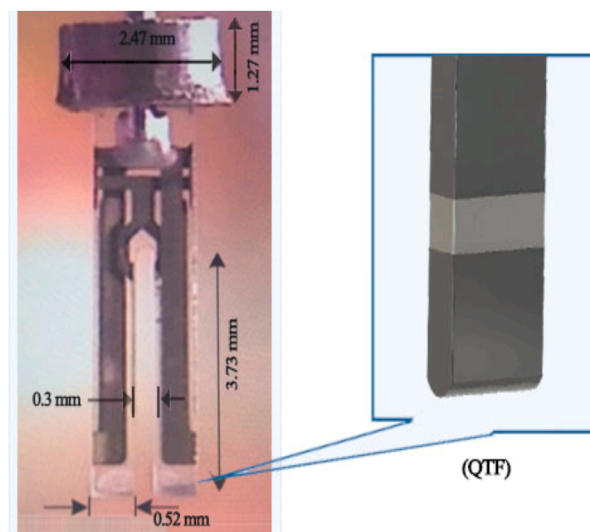


Fig. 2. Schematic illustrating a standard QTF sensor (Alanazi et al., 2021).



in human hepatocytes after 48 h of gamma-ray irradiation. They observed an increase in both DSBs and SSBs proportionate to the irradiation doses, with DSBs being more prevalent. After 24 h, partial repair occurred, covering up to 15 % chromatid DNA breaks and nearly 50 % stained chromatids. Repairing isochromatid breaks remained challenging (Jia, 2021). If damage signals persist despite initial repair mechanisms, cells do not replicate damaged DNA and prioritize mechanisms such as cell death, cell cycle arrest, or senescence (Yousefzadeh et al., 2021). The transcriptional regulator p53, activated by ATM, coordinates these responses by interacting with signal transduction and cell cycle regulation pathways. In severe DNA damage that is difficult to repair, cells can activate checkpoints and initiate apoptosis (van de Kamp, 2021).

#### (1) HR repair.

This modeling method facilitates the accurate repair of DSBs through NHEJ. At the same time, HR involves obtaining the correct sequence from intact DNA or initiating the resection of damaged DNA ends by nucleases to restore strand integrity. CtIP and Mre11 proteins are crucial for generating single-stranded DNA from DSB ends (Santivasi and Xia, 2014). The primary, slower DSB repair pathway during the S and G2 phases uses an undamaged sister chromatid as a repair template, ensuring error-free DNA restoration. Additionally, the HR pathway identifies DNA damage, activating the Mre11-Rad50-NBS1 (MRN) complex and ATM through BRCA1 proteins. ATM phosphorylates and activates BRCA1, initiating cell cycle checkpoints. Subsequently, BRCA1 indirectly interacts with Rad51, facilitating the exchange of damaged strands and their pairing with a homologous template to locate sequences, ultimately restoring the original double strand by elongating and ligating the broken strands (Penninckx, 2021).

#### (2) NHEJ repair.

NHEJ is an alternative repair pathway for various DSBs, though it exhibits lower fidelity than HR. Using Ku70 and Ku80 proteins (XRCC5), NHEJ protects damaged DNA from exonuclease enzymes and recombines DSB ends without requiring homologous sequences. This method ensures accurate repair without a homologous template. Ku70 and Ku80 identify DSBs and recruit proteins to the breakpoints, forming an active DNA-PK holoenzyme. Nucleases are subsequently recruited to expose DNA ends and digest nucleotides from both strands. NHEJ is a DNA repair system and a checkpoint activator (Lin and Yanti, 2015). Eventually, a stable complex involving DNA ligase I is formed, which binds the two repaired DNA ends facilitated by enhanced DNA-PK activity. This enhancement increases resistance to IR in various cancer cells, including glioblastoma multiforme (GBM), the most common primary brain malignancy. Therefore, leveraging a tumor's deficiency in NHEJ for treatment planning may be a viable strategy (Penninckx, 2021).

### 3. Results

In this study, we detected DNA denaturation by measuring DNA damage using a QTF sensor, represented by  $\Delta f$ . DNA was monitored before, during, and after irradiation for 60 min using the QTF controller. The data were analyzed using Origin Lab v.6 software (Wellesley Hills, MA, USA) on the Windows Operating System, with the mean calculated every 5 min to achieve the best fit, as illustrated in Figs. 3 and 4.

#### 3.1. Before the irradiation stage

Initially, pure DNA samples were prepared using commercial genomic DNA obtained at 2-ng/ $\mu\text{L}$  (60  $\mu\text{L}$  in total) concentration, purchased from Applied Biosystems Company. Additionally, DI water and quartz tuning forks were acquired from FOURIEN (Edmonton, AB, Canada), as depicted in Fig. 2. Subsequently, a second sample was prepared by mixing pure DNA with deionized water to create a DNA solution (60  $\mu\text{L}$  in total). Finally, a sample containing only water (60  $\mu\text{L}$ ) was prepared. Subsequently, the experimental setup was modified by removing the hermetic casing of the QTF to improve contact with the

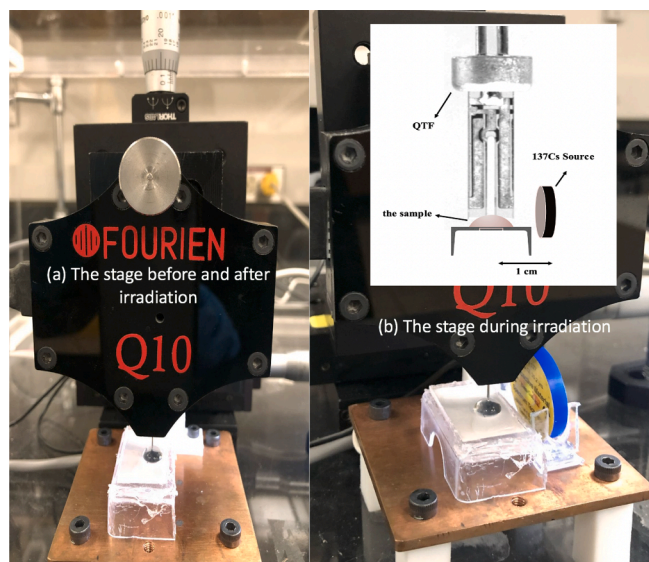


Fig. 3. Experimental setup geometry. (a) The stage before and after irradiation, and (b) the stage during irradiation.

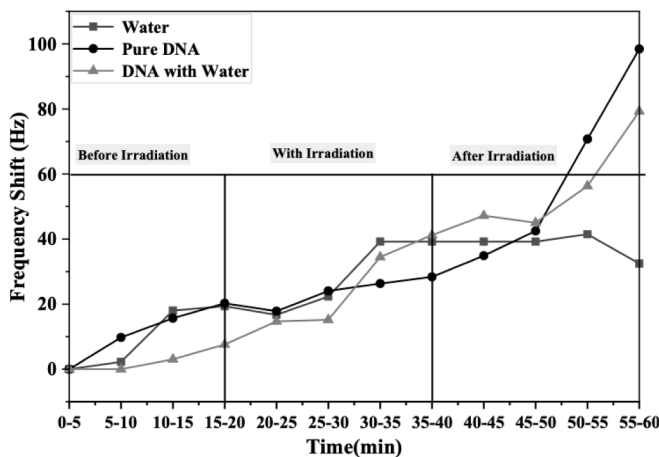


Fig. 4. Variations in the frequency spectra of DNA damage and the quantity of each type of DNA damage over time, including periods before, during, and after gamma irradiation, as measured by the QTF sensor.

sample and observe DNA behavior. During sample recognition, the fork functioned normally, facilitating signal transduction from the conventional biosensors in the form of frequency shifts in each sample over 20 min. Fig. 5 shows a slight increase observed in the investigated samples.

#### 3.2. During the irradiation stage

In this study, the samples were exposed to radiation from a synthetic radioactive nuclide, cesium-137, which has a half-life of 30.2 years and a current activity of 5  $\mu\text{Ci}$ . The gamma source was positioned directly adjacent to the QTFs at a distance of 1 cm. The dose rate was  $\sim 1.5 \mu\text{Gy}/\text{min}$ , generating gamma rays with an energy of 662 keV. At different time intervals corresponding to various doses, the samples were exposed at room temperature (25  $^{\circ}\text{C}$ ) in the chamber for 20 min. The samples were positioned 1 cm away from the cesium-137 source, parallel to the direction of the gamma source, as depicted in Fig. 3. During this phase, the fork was immersed in the samples, after which we exposed the samples to gamma radiation from a cesium-137 source. We observed deformation owing to DNA damage and investigated the effects of gamma radiation on DNA strand breaks in our samples. The baseline

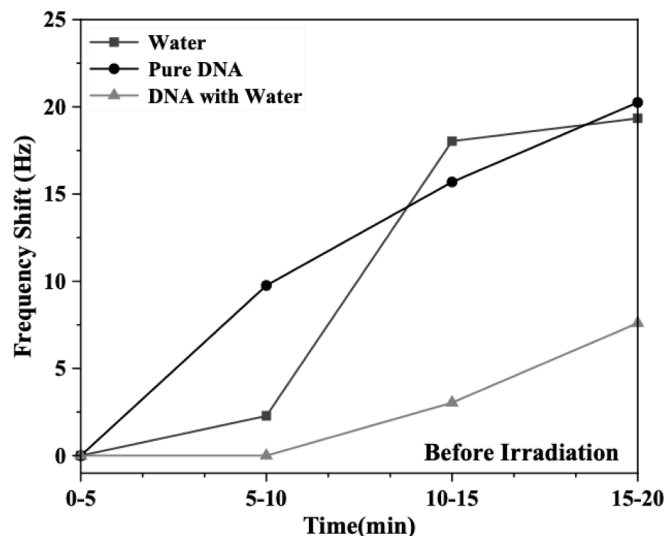


Fig. 5. Frequency shifts of DNA with and without water, as well as water alone, monitored over a 20-min period before exposure to gamma radiation, with measurements taken every 5 min.

level of DNA oxidative damage was determined by calculating the difference in frequency moments before and after irradiation at 20 min, represented as the sensitive site of the fork frequency shift.

Fig. 6 shows the DNA damage frequency spectra results with and without water, including results for water alone. The results demonstrate an increase in frequency from ~ 15  $\mu\text{Gy}$  to ~ 22.5  $\mu\text{Gy}$  at an exposure time of ~ 10 min; further exposure for 20 min increased the frequency to ~ 30  $\mu\text{Gy}$ . Notably, the amount of DNA damage increased after ~ 5 min of exposure: 7.5  $\mu\text{Gy}$  in the order of water, DNA, and DNA with water, resulting in  $\Delta f$  values of ~ 16.71, 17.83, and 14.7 Hz, respectively. However, after 10-min irradiation with doses of 7.5–15  $\mu\text{Gy}$ , the  $\Delta f$  observed were ~ 22.34, 24.05, and 15.21 Hz for water, DNA, and DNA with water, respectively. Finally, after 20 min (dose = 7.5–30  $\mu\text{Gy}$ ), the frequency shifts were ~ 39.21, 28.37, and 41.23 Hz for water, DNA, and DNA with water, respectively. Furthermore, a substantial increase in DNA strand breaks was observed, as indicated by the shifts in fork frequencies, with absorbed doses starting at 7.5  $\mu\text{Gy}$  in 5 min, increasing to 15  $\mu\text{Gy}$  during exposure, and peaking at 30  $\mu\text{Gy}$ .

Moreover, Fig. 6 and Table 1 show the recorded frequency shifts, highlighting a clear correlation between dose increments and observed frequency shifts during radiation exposure, reflecting the extent of

Table 1

Frequency shifts observed during gamma radiation exposure at intervals of 20–40 min, and frequency shifts recorded after exposure at intervals of 40–60 min.

Stage	Time (min)	Frequency shift (Hz)		
		Water	Pure DNA	DNA with Water
with gamma radiation	(20–25)	16.71	17.83	14.7
	(25–30)	22.34	24.05	15.21
	(30–35)	39.21	26.33	34.47
	(35–40)	39.21	28.37	41.23
after gamma radiation	(40–45)	39.21	34.89	47.2
	(45–50)	39.21	42.5	45.03
	(50–55)	41.49	70.75	56.32
	(55–60)	32.48	98.45	79.28

DNA’s response to radiation. Thus, by monitoring the fork’s frequency behavior in DNA damage during exposure, we conducted experiments using several media: DNA alone, DNA combined with deionized water, and just water under identical conditions. According to Table 1, variations in  $\Delta f$  were observed, attributed to increased DNA damage.

After 10 min of exposure, the damage observed for water showed a frequency shift ranging from  $\Delta f \sim 16.7$  to 39.2 Hz. The frequency shift for DNA in aqueous solution ranged from  $\Delta f \sim 14.7$  to 34.4 Hz, indicating a noticeable increase. Therefore, this specific dose was selected as the maximum experimental dose. Consequently, in the presence of water, the DNA’s response to irradiation significantly increased, with the frequency increasing from  $\Delta f \sim 28.37$  to 41.23 Hz, nearly doubling its initial value. The examinations further indicated that, while the sample experienced significant frequency changes, these changes were comparatively less pronounced than those observed when the DNA was present alone. Consequently, in the presence of water, the DNA’s response to irradiation significantly increased, with the frequency increasing from  $\Delta f \sim 28.37$  to 41.23 Hz, approximately doubling its initial value. The examinations further indicated that, while the sample experienced significant frequency changes, these changes were less pronounced than those observed when the DNA was present alone. We attributed the shift in frequency to the gamma-ray interaction with water. In these interactions, water demonstrates indirect effects by generating highly reactive free radicals— $\text{H}\cdot$ ,  $\text{OH}\cdot$ ,  $\text{H}^+$ , and  $\text{OH}^-$ . These radicals disperse widely, causing more extensive DNA damage. This increase in frequency was observed after 10 min of exposure, suggesting that indirect reactions are more damaging compared to direct exposure of pure DNA. Furthermore, no repair was observed in the presence of DNA alone or with water based on this observation. This finding underscores the need to discuss this in the following stage.

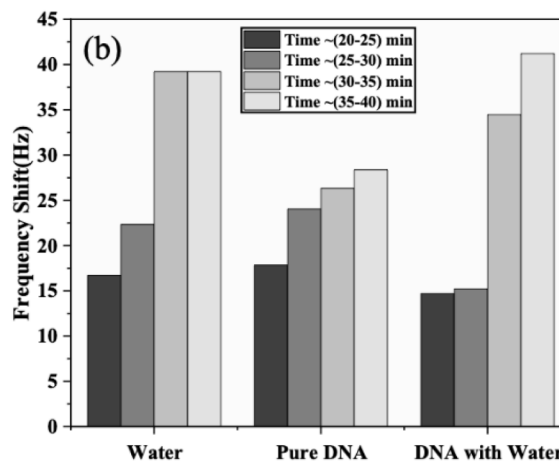
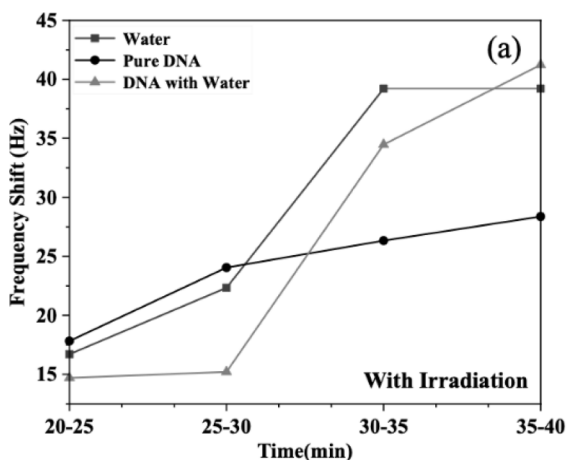


Fig. 6. DNA strand breaks induced by gamma irradiation without and with water over a 20-min exposure period. (a) From 20 to 40 min, with measurements recorded every 5 min, and (b) the progressive response of each sample with frequency shifts upon exposure to gamma radiation.

### 3.3. DNA repair stage

In the final stage, after the completion of the irradiation process as described earlier, the cesium-137 source was removed from the chamber after a 20-min exposure. This step was taken to observe the repair of DNA once the effects of radiation subsided. The fork was immersed in the same samples without the gamma radiation source, and the frequencies were recorded for DNA following exposure to gamma radiation doses ranging from 7.5 to 30  $\mu\text{Gy}$ . The findings indicated an initial increase in frequency expression levels immediately after exposure, followed by a decline in DNA with water at 60 min. Subsequently, DNA and water exhibited an increase in frequency shift,  $\Delta f \sim 79$  Hz and  $\Delta f \sim 98$  Hz, respectively, as detailed in Table 1. As depicted in Fig. 7, the residual damage was assessed immediately after irradiation (20 min) for each damage period and plotted against the postirradiation time. However, the frequency shift remained stable for water at  $\sim 39.21$  Hz for 10 min, increased to  $\sim 41$  Hz, and then decreased to  $\sim 32$  Hz. This shift is attributed to gamma rays impacting the water. The observed increase in frequencies of direct and indirect repair reactions indicates that gamma radiation caused complete DNA damage, which was challenging-to-repair owing to the lack of a suitable environment. This finding suggests that the DNA repair context did not significantly influence DNA responses in this study. However, the roles of DNA damage response proteins, such as *gH2AX*, *ATM*, *53BP1*, *RAD51*, and the *MRE11/RAD50/NBS1* complex at DNA damage sites, could greatly influence interpretations, particularly in genes related to recombination near DSB. This influence contributes to the repair mechanisms under investigation. Despite processing via recombination through BER enzymes in living cells, certain damages may persist, potentially leading to significant genetic consequences such as the induction of mutations. Indeed, there is mounting evidence that deficiencies in DNA repair stem from insufficient DNA damage response proteins. We performed a comparable experiment using water as a medium to investigate DNA damage response and repair under the *ex vivo* conditions used in this study. Water was irradiated under identical conditions as DNA, followed by removal from the radiation source to observe fork shift frequencies. Initially, the frequency increased upon exposure and subsequently decreased during the repair phase. These observations are indicators of damage and repair. Thus, our findings provide a biological rationale for the substantial increase in DNA damage predicted by a dose-response relationship and assessed through a sensitive assay.

## 4. Discussion

The study distinguishes between direct and indirect DNA damage

resulting from gamma-ray exposure. Fork frequency is an indicator of DNA damage in this experiment. Levels of DNA strand breaks and oxidative base damage are quantified as fork frequency-sensitive sites by QTF, enabling monitoring of radical effects on DNA. More strand breaks were observed in DNA compared to water, where OH-radicals cause DNA damage. Levels of DNA strand breaks substantially increased from  $\sim 7.5$  to 30  $\mu\text{Gy}$  during the exposure stage at a low-dose rate; however, similar differences were not observed when the dose increased from 7.5 to 15  $\mu\text{Gy}$  (Table 1). Overall, the duration of damage frequency persisted longer after source removal than during radiation exposure. Fig. 4 illustrates differences in frequency characteristics before and after radiation exposure, highlighting results at the lowest dose. Further examination of gamma-ray irradiation revealed that while a single exposure at 7.5  $\mu\text{Gy}$  initially did not cause significant DNA damage, a slight increase was observed with higher doses. These findings indicate that the dose and the rate of dose adjustments influence the frequency of bond-breaking. Gamma radiation is likely to induce DNA damage directly or indirectly by generating reactive oxygen species, resulting in oxidative lesions. Antonelli (2015) demonstrated that low radiation levels typically induce DNA damage, with the highest frequencies observed during the tested radiation periods. While recognizing that IR can cause DSBs at doses used in medical imaging, Siegel et al. (Siegel, 2017) do not fully understand the effects of this damage. However, investigations by Lo brich et al. (Löbrich, 2005) aimed to determine whether DNA strands could be reconnected following exposure to IR.

In our study, frequencies remained consistent across pure DNA, DNA in aqueous solution, and water during the presource stage. However, at the postsource stage, frequencies remained stable for  $< 45$  min but showed a slight increase at 45–60 min compared to during exposure. These results suggest that the frequency was unaffected by the dose rate but was primarily influenced by postirradiation effects. After 45 min, no significant change was observed in DNA repair for both pure DNA ( $\Delta f \sim 98.45$  Hz) and DNA in aqueous solution ( $\Delta f \sim 79.28$  Hz), indicating their intrinsic repair capacity under suitable conditions, facilitated by DNA repair proteins at damage sites. Regulatory mechanisms control DNA damage response and repair, limiting the predictive efficacy of any single biological process. Contrarily, water showed a decrease and subsequent recovery in repair ( $\Delta f \sim 32.48$  Hz) under similar conditions.

We explored the impact of gamma radiation from cesium-137 on DNA in aqueous solution and pure form using biosensors. Our goal was to elucidate the fundamental mechanisms of radiosensitization and anticipate the effects of DNA damage. However, our study has limitations. While we confirmed DNA damage induced by the radiation dose in the second stage, we did not assess the potential for DNA repair owing to the absence of a conducive environment. Future research should address

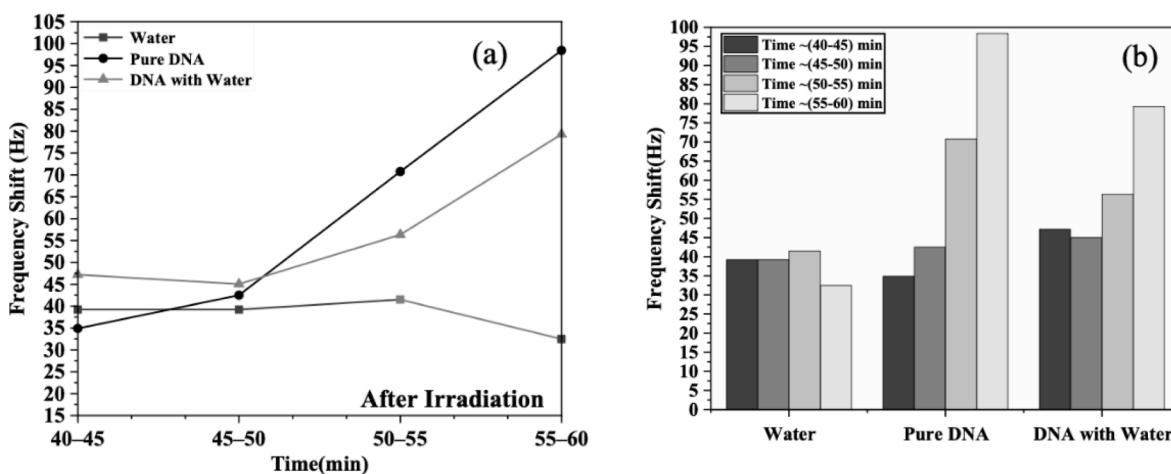


Fig. 7. Frequency shifts of DNA with and without water, and in just water, following exposure to gamma radiation. (a) Between 40 and 60 min, with measurements recorded every 5 min, and (b) the gradual response of each sample with frequency shifts after exposure to gamma radiation.



this gap by providing such an environment to facilitate DNA self-restoration postradiation exposure. Nonetheless, our findings suggest that QTFs are promising in elucidating frequency shifts caused by DNA damage from gamma radiation, offering avenues for personalized cancer treatments.

## 5. Conclusion

In summary, this study used QTF as a biosensor to quantify DNA damage induced by direct and indirect radiation effects of water on DNA. Analysis of the irradiation process indicated a substantial increase in overall damage attributed to water compared to DNA alone. While the irradiation phase showed higher frequency shifts indicating DNA damage in the presence of water, this effect was significantly less pronounced than that observed with direct DNA damage. Thus, it is inferred that this behavior resulted from the initiation of indirect damage processes by excited water molecules and hydroxyl radicals.

Finally, postirradiation DNA damage increased with direct and indirect repair reactions, highlighting the extensive damage induced by gamma radiation. Furthermore, effective repair requires the presence of DNA damage response proteins in the medium, complicating the DNA repair process. Thus, these findings confirm the potential of QTFs as sensitive and promising tools in medical and biological applications, offering a simplified model for assessing DNA damage during direct and indirect reactions with gamma radiation.

## CRedit authorship contribution statement

**Reem Alanazi:** Conceptualization, Formal analysis, Investigation, Writing – original draft, Writing – review & editing. **Khaled Alzahrani:** Formal analysis, Investigation, Methodology. **Khalid E. Alzahrani:** Investigation, Visualization, Writing – review & editing. **Nadyah Alanazi:** Conceptualization, Formal analysis, Visualization, Writing – review & editing. **Abdullah N. Alodhayb:** Conceptualization, Investigation, Supervision, Visualization, Writing – review & editing.

## Declaration of competing interest

The authors declare that they have no known competing financial interests or personal relationships that could have appeared to influence the work reported in this paper.

## Acknowledgment

The authors extend their appreciation to the Deputyship for Research and Innovation, Ministry of Education in Saudi Arabia for funding this research work through the project no. (IFKSUOR3–231–4).

## References

- Alanazi, Nadyah, et al., 2021. Quartz tuning fork sensor based dosimetry for sensitive detection of gamma radiation. *Materials* 14 (22), 7035. <https://doi.org/10.3390/ma14227035>. MDPI AG.
- Alanazi, Nadyah, et al., 2022. Review—measurements of ionizing radiations using micromechanical sensors. *ECS J. Solid State Sci. Technol.* 11 (5), 057001. <https://doi.org/10.1149/2162-8777/ac6f20>. The Electrochemical Society.
- Alanazi, Nadyah, et al., 2023. Effect of gold nanoparticle radiosensitization on DNA damage using a quartz tuning fork sensor. *Micromachines* 14 (10), 1963. <https://doi.org/10.3390/mi14101963>. MDPI AG.
- Alexandros, Georgakilas, G., 2020. Role of DNA damage and repair in detrimental effects of ionizing radiation. *Radiation* 1 (1), 1–4. <https://doi.org/10.3390/radiation1010001>. MDPI AG.
- Alodhayb, A., 2020. Quartz tuning fork, a low-cost orthogonal measurement tool for the characterization of low-volume liquid reagents. *Measurement* 152, 107313. <https://doi.org/10.1016/j.measurement.2019.107313>. Elsevier BV.
- Alshammari, Abeer, et al., 2020. Detection of chemical hostguest interactions using a quartz tuning fork sensing system. *IEEE Sens. J.* 20 (21), 12543–12551. <https://doi.org/10.1109/jsen.2020.3002347>. Institute of Electrical and Electronics Engineers (IEEE).
- Antonelli, F., et al., 2015. Induction and Repair of DNA DSB as Revealed by H2AX phosphorylation foci in human fibroblasts exposed to low- and high-LET radiation:

- relationship with early and delayed reproductive cell death. *Radiat. Res.* 183 (4), 417–431. <https://doi.org/10.1667/rr13855.1>. Radiation Research Society.
- Blimkie, Melinda S.J., et al., 2014. Repair of DNA double-strand breaks is not modulated by low-dose gamma radiation in C57BL/6J Mice. *Radiation Res. Soc.* 181 (5), 548. <https://doi.org/10.1667/rr13324.1>. Radiation Research.
- Budak, M., 2020. Radiation, and DNA methylation mechanisms. *DNA Methylation Mechanism*. <https://doi.org/10.5772/intechopen.92189>. IntechOpen.
- Chatterjee, Nimrat, Walker, Graham C., 2017. Mechanisms of DNA damage, repair, and mutagenesis. *Environ. Mol. Mutagen.* 58 (5), 235–263. <https://doi.org/10.1002/em.22087>. Wiley.
- de la Fuente Rosales, L. A Monte Carlo Study of the Direct and Indirect DNA Damage Induced by Ionizing Radiation, 2018.
- Duncan, James R., Swensen, Stephen J., 2016. DNA repair after exposure to ionizing radiation is not error-free. *Radiology* 280 (1), 322–323. <https://doi.org/10.1148/radiol.2016152738>. Radiological Society of North America (RSNA).
- Faraj Akram, K., et al., 2011. Effect of X- and Gamma Rays on DNA in Human Cells. *Eur. J. Sci. Res.* 53 (3), 470–476.
- Gong, Liyun, et al., 2021. Application of radiosensitizers in cancer radiotherapy. *International Journal of Nanomedicine* 1083–1102.
- Iin, K., & Yanti, L. (2015).  $\gamma$ -H2AX dan Potensinya untuk Biomarker Prediksi Toksisitas Radiasi pada Radioterapi. In Seminar Nasional Keselamatan Kesehatan dan Lingkungan dan Pengembangan Teknologi Nuklir (pp. 188-194). PTKMR.
- Jia, Chengyou, et al., 2021. The role of DNA damage induced by low/high dose ionizing radiation in cell carcinogenesis. *Exploratory Research and Hypothesis in Medicine* 000 (000), 000. <https://doi.org/10.14218/erhm.2021.00020>. Xia and He Publishing.
- Kaleli-Can, Gizem, et al., 2021. Development of mass sensitive sensor platform based on plasma polymerization technique: quartz tuning fork as transducer. *Appl. Surf. Sci.* 540, 148360. <https://doi.org/10.1016/j.apsusc.2020.148360>. Elsevier BV.
- Kundu, S., et al., 2020. Direct damage of deoxyadenosine monophosphate by low energy electrons probed by x-ray photoelectron spectroscopy. *The Journal of Physical Chemistry B, American Chemical Society (ACS)*. <https://doi.org/10.1021/acs.jpcc.9b08971>.
- Löblich, Markus, et al., 2005. In vivo formation and repair of DNA double-strand breaks after computed tomography examinations. *Proc. Natl. Acad. Sci.* 102 (25), 8984–8989. <https://doi.org/10.1073/pnas.0501895102>. Proceedings of the National Academy of Sciences.
- McKee, A.D., et al., May 2019. Low energy secondary electron induced damage of condensed nucleotides. *J. Chem. Phys.* 150 (20), 204709 <https://doi.org/10.1063/1.5090491>. AIP Publishing.
- Moreels, Marjan, et al. "Stress and Radiation Responsiveness. In: Choukèr, A. (eds) Stress Challenges and Immunity in Space". 2020. Doi: 10.1007/978-3-030-16996-1\_20. Springer, Cham.
- Nikjoo, P. O'Neill, D. T. Goodhead, H. Computational Modelling of Low-energy Electron-induced DNA Damage by early physical and chemical events." *International Journal of Radiation Biology*, 71, (5), Jan. 1997, pp. 467–83. Doi: 10.1080/095530097143798. Informa UK Limited.
- Penninckx, Sébastien, et al., 2021. Quantification of Radiation-induced DNA double strand break repair foci to evaluate and predict biological responses to ionizing radiation. *NAR Cancer* 3 (4). <https://doi.org/10.1093/narcan/zcab046>. Oxford UP (OUP).
- Ptasińska, Sylwia, et al., 2008. X-ray Induced Damage in DNA Monitored by X-ray photoelectron spectroscopy. *J. Chem. Phys.* 129 (6), 065102. <https://doi.org/10.1063/1.2961027>. AIP Publishing.
- Anwar Qasim, Ahmed, et al. "The Impact of Gamma Ray on DNA Molecule." *International Journal of Radiology and Radiation Oncology*, 6, (1), May 2020, pp. 011–13. Doi: 10.17352/ijrro.000038. Peertechz Publications Private Limited.
- Rosenberg, R.A., et al., 2014. The relationship between interfacial bonding and radiation damage in adsorbed DNA. *Phys. Chem. Chem. Phys.* 16 (29), 15319–15325. <https://doi.org/10.1039/c4cp01649a>. Royal Society of Chemistry (RSC).
- Rousseau, Roman, et al., 2019. Quartz tuning fork resonance tracking and application in quartz enhanced photoacoustics spectroscopy. *Sensors* 19 (24), 5565. <https://doi.org/10.3390/s19245565>. MDPI AG.
- Santivasi, Wil L., Xia, Fen, 2014. Ionizing radiation-Induced DNA damage, response, and repair. *Antioxid. Redox Signal.* 21 (2), 251–259. <https://doi.org/10.1089/ars.2013.5668>. Mary Ann Liebert Inc.
- Shimoda, Y., Uno, T., 1988. Radiation-induced frequency changes in quartz oscillators. *Jpn. J. Appl. Phys.* 27 (S1), 114. <https://doi.org/10.7567/jjaps.27s1.114>. IOP Publishing.
- Siegel, Jeffrey A., et al., 2017. Dose optimization to minimize radiation risk for children undergoing CT and nuclear medicine imaging is misguided and detrimental. *J. Nucl. Med.* 58 (6), 865–868. <https://doi.org/10.2967/jnumed.117.195263>. Society of Nuclear Medicine.
- Sudprasert, Wanwisa, et al., 2006. Effects of Low-dose Gamma Radiation on DNA Damage, Chromosomal Aberration and Expression of Repair Genes in Human Blood Cells. *Int. J. Hyg. Environ. Health* 209 (6), 503–511. <https://doi.org/10.1016/j.ijheh.2006.06.004>. Elsevier BV.
- van de Kamp, Gerarda, et al., 2021. DNA double strand break repair pathways in response to different types of ionizing radiation. *Front. Genet.* 12 <https://doi.org/10.3389/fgene.2021.738230>. Frontiers Media SA.
- Vogelhuber-Brunnmaier, Thomas, et al., 2019. Fluid Sensing Using Quartz Tuning Forks—Measurement Technology and Applications. *Sensors* 19 (10), 2336. <https://doi.org/10.3390/s19102336>. MDPI AG.
- Wang, Hui, et al., 2019. "Hypoxic Radioresistance: Can ROS Be the Key to Overcome It?" *Cancers*, 11, (1), Jan. 2019, p. 112. Doi: 10.3390/cancers11010112. MDPI AG.

- Xiao, Fangxing, 2013. Cleavage enhancement of specific chemical bonds in DNA by cisplatin radiosensitization. *J. Phys. Chem. B* 117 (17), 4893–4900. <https://doi.org/10.1021/jp400852p>. American Chemical Society (ACS).
- Xu, Xu, et al., 2019. Direct Observation of Damage Clustering in Irradiated DNA With Atomic Force Microscopy. *Nucleic Acids Res.* 48 (3), e18. <https://doi.org/10.1093/nar/gkz1159>. Oxford UP (OUP).
- Yousefzadeh, M., Henpita, C., Vyas, R., Soto-Palma, C., Robbins, P., & Niedernhofer, L. (2021, January 29). DNA damage—how and why we age?, 10. Doi: 10.7554/elife.62852. ELife.
- Zhang, Xiaofei, et al., 2018. Sensing performance analysis on quartz tuning fork-probe at the high order vibration mode for multi-frequency scanning probe microscopy. *Sensors* 18 (2), 336. <https://doi.org/10.3390/s18020336>. MDPI AG.